Chinese Journal of Aeronautics, (2014),27(6): 1527–1537

Chinese Society of Aeronautics and Astronautics
& Beihang University

Chinese Journal of Aeronautics

cja@buaa.edu.cn
www.sciencedirect.com

PI controller relay auto-tuning using delay and phase margin in PMSM drives

Wang Lina [a], Xiao Kun [b,*], Liliana de Lillo [c], Lee Empringham [c], Pat Wheeler [c]

[a] *School of Automation Science and Electrical Engineering, Beihang University, Beijing 100091, China*
[b] *Material and Supervision Department, State Grid DC Project Construction Company Limited, Beijing 100052, China*
[c] *Department of Electrical and Electronic Engineering, University of Nottingham, Nottingham NG7 2RD, UK*

Received 13 October 2013; revised 29 June 2014; accepted 5 August 2014
Available online 18 October 2014

KEYWORDS

Auto-tuning;
EMA;
Matrix converters;
PI control;
PMSM

Abstract This paper presents an auto-tuning method for a proportion plus integral (PI) controller for permanent magnet synchronous motor (PMSM) drives, which is supposed to be embedded in electro-mechanical actuator (EMA) control module in aircraft. The method, based on a relay feedback with variable delay time, explores different critical points of the system frequency response. The Nyquist points of the plant can then be derived from the delay time and filter time constant. The coefficients of the PI controller can then be obtained by calculation while shifting the Nyquist point to a specific position to obtain the required phase margin. The major advantage of the auto-tuning method is that it can provide a series of tuning results for different system bandwidths and damping ratios, corresponding to the specification for delay time and phase margin. Simulation and experimental results for the PMSM controller verify the performance of both the current loop and the speed loop auto-tuning.

1. Introduction

The permanent magnet synchronous motor (PMSM) has received increasing acceptance in industrial applications, due to its features of high efficiency, low noise, high performance and robustness. It plays a fundamental role in manufacturing automation, such as robotics, hybrid vehicles, electric scooters, elevators and applications in aircraft.[1,2] A high-performance PMSM drive generally requires an estimation of the motor parameters, such as armature inductance and resistance, as well as moment of inertia of the whole system including the motor and the load. Any variation of parameters such as the moment of inertia will affect and degrade the drive's performance.[3] So it is important to have the correct value while performing the motor control. It is not an easy task however to obtain a good estimation of all the required parameters in a motor drive system.

One of the most popular controllers is the proportional plus integral (PI) type, which is widely used in the field-orientated control of PMSMs. Since it is often difficult to measure the PMSM parameters, manipulation tuning is a frequently-used way to determine the PI coefficient instead of theoretical

* Corresponding author. Tel.: +86 10 63416872.
E-mail address: kun-xiao@sgcc.com.cn (K. Xiao).

Peer review under responsibility of Editorial Committee of CJA.

Production and hosting by Elsevier

http://dx.doi.org/10.1016/j.cja.2014.10.019

calculations. It takes even experienced engineers time and effort to regulate the PI coefficients to guarantee good performance. As a result, there exists a growing demand for auto-tuning of the PI controller, without knowing the varying operating parameters. Auto-tuning is a powerful control technique used to solve the above problem and is based on an adaptive estimation algorithm.[4,5]

During the past decades, the theory of auto-tuning has developed in a variety of directions. The pioneering work can be traced to the 1940s. Ziegler et al.[6] tuning relations and Cohen and Coon[7] tuning rules are among the earliest published methods. Since then, the subject has been extensively explored and it is still under investigation.[8–10] The popularity of these controllers has led to research on tuning methods, resulting in hundreds of publications on this topic. Tuning relations based on error criteria, as well as more recent model-based tuning rules such as internal model control (IMC) and direct synthesis,[11] offer improvements over earlier tuning methods. Tuning rules also exist for unstable processes[12] as well as for tuning in the presence of plant-model mismatch. In Ref. [13] a sensorless vector-control design and tuning strategy is introduced based on state observer, phase-locked loop, tracking controller, etc. Many developments have been reported to extend the relay auto-tuning method. It transpires that more accurate information on process dynamics can be obtained from the same relay test with the help of new identification techniques and can be used to improve the tuning of PI controllers.[14–18]

In this paper, an auto-tuning method based on relay feedback for both current loop and speed loop is presented. By specifying the delay time and phase margin, the system bandwidth and damping ratio can be regulated. Firstly, the modeling of the PMSM and the PI controller is introduced, which shows the connection of the PI controller settings and system performance. Secondly, the proposed relay auto-tuning strategy is presented. The changes in the delay time and the phase margin cause a shifting of the plant's Nyquist point to the position of the specific phase margin on the unit circle in the s-domain, from which the tuning formulas are derived. The qualitative analysis is illustrated and simulated, in order to show the connection between the settings of the delay time/phase margin and the system response. Finally, experiments are carried out in a electro-mechanical actuator (EMA) for PMSM and permanent-magnet flux-switching machine (PMFSM). In both cases an Indirect Matrix Converter is implemented to drive the machines. The experimental results show the validity of the proposed auto-tuning method.

2. Modeling of the drive system

2.1. Electrical and mechanical model of PMSM

The control block diagram for the current loop and the speed loop can be generally derived. The current loop of a PMSM can be simplified as shown in Fig. 1. Where L_s is the inductance of surface mounted PMSM; R_s is the resistance of surface mounted PMSM; i is the current to be controlled and i_{ref} is the reference current. Assume that $L_q = L_d = L_s$ in a surface mounted PMSM, where L_q is the q-axis inductance, and L_d is the d-axis inductance. The back-electromotive force (EMF) equals $(L_d\omega_r i_d + \omega_r\psi_f)$ for the q-axis current loop

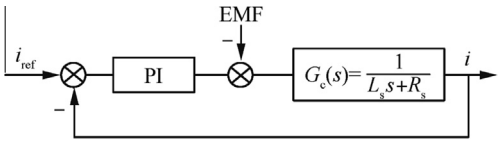

Fig. 1 Simplified model of current loop of PMSM.

whereas $(-L_q\omega_r i_q)$ for the d-axis current loop, where ω_r is the mechanical rotating speed, Ψ_f is the excitation flux, i_q is the q-axis current, and i_d is the d-axis current. The plant in the current loop is finally simplified as a first-order system with the time constant L_s/R_s.[19] In the practical servo system, the power converter delays the current response at least one pulse width modulation (PWM) period. It is neglected in Fig. 1 and considered as a part of the current loop transfer function $G_c(s)$ in the paper, and the delay could be tuned by means of the method proposed.

The speed loop can be simplified as shown in Fig. 2. $G_{cl}(s)$ represents the current closed loop transfer function including the power converter, the dead-time and the PMSM current loop. T_L represents the load torque, and ω is the speed to be controlled while ω_{ref} is the reference speed. Considering that the time constant in the current loop is much smaller than the one in the speed loop, $G_{cl}(s)$ is assumed to be 1 to simplify the analysis. This is not quite accurate for most system modelings. However in this paper, it is not based on an accurate modeling and allows the simplification to assume it as a part of the plant. Then the plant in the speed loop can be assumed as a first-order system with the time constant J/B, where J is the total inertia of PMSM, and B is the friction.

2.2. PI calculation based on system bandwidth and damping ratio

The PI controller in the time domain has the expression as

$$u(t) = K_p e(t) + K_i \int e(t)\mathrm{d}t \tag{1}$$

where K_p and K_i are the proportional and the integral coefficients, respectively; $e(t)$ is the error between the reference and the feedback signal.

In the s-domain, the PI controller will be expressed by Eq. (2) as

$$P_{PI}(s) = K_p + \frac{K_i}{s} = K_p\left(1 + \frac{1}{T_i s}\right) \tag{2}$$

with $T_i = K_p/K_i$.

Considering that both the plants of the current loop and the speed loop are first-order systems, they can be represented in a normalized form

$$P(s) = \frac{k}{s+p} \tag{3}$$

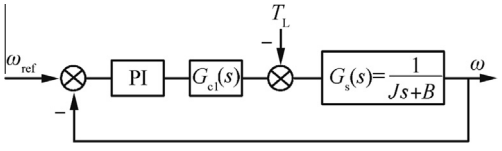

Fig. 2 Simplified model of speed loop of PMSM.

where k and p are related to the electrical parameters (resistance and inductance) and mechanical parameters (inertia and friction).

Then the open-loop transfer function of the current loop and the speed loop in Figs. 1 and 2 can be represented as

$$G(s) = \frac{k(K_p s + K_i)}{s(s+p)} \tag{4}$$

The corresponding closed-loop transfer function is

$$\Phi(s) = \frac{k(K_p s + K_i)}{s^2 + (p + K_p k)s + K_i k} \tag{5}$$

Thus the closed current loop and the closed speed loop transfer function are second-order systems, in which the damping ratios ς and system bandwidths ω_n are

$$\begin{cases} 2\varsigma\omega_n = p + K_p k \\ \omega_n^2 = K_i k \end{cases} \tag{6}$$

If the electrical and mechanical parameters of a PMSM are well-known, K_p and K_i can be immediately calculated from Eq. (6). However, it is not an easy task to measure the parameters of a PMSM. Moreover, the parameters change if the temperature increases while a PMSM is operating. Also, the variation of the load inertia will degrade the drive's performance. These factors increase the difficulties of the theoretical calculation of the PI coefficients. In this paper, the relay auto-tuning control strategy is investigated to find a way to solve the problem described above.

3. Proposed auto-tuning scheme

3.1. Basic issues of relay auto-tuning theory

The relay auto-tuning scheme focuses on the idea that most systems oscillate under the relay control.[20] Consider the closed loop system in Fig. 3, the relay output $u(t)$, the system reference output $y_{ref}(t)$ and the system output $y(t)$ are shown in Fig. 4, and the whole oscillating procedure is explained in Ref. [19]. Eventually the output is driven to a steady oscillation state, which carries the information of the amplitude and the frequency of the cross-point between the plant Nyquist curve and the negative real axis in the s-domain. The cross-point is defined as the critical point.

A describing function approximation is employed[21] and the ultimate gain K_u and the ultimate period T_u are derived as[6]

$$\begin{cases} K_u = N(a) = \frac{4u}{\pi a} \\ T_u = \frac{2\pi}{\omega_u} \end{cases} \tag{7}$$

where $N(a)$ is the describing function of the relay; u is the amplitude of the relay output; a is the amplitude of the plant

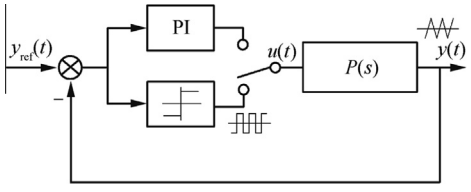

Fig. 3 Relay auto-tuning scheme.

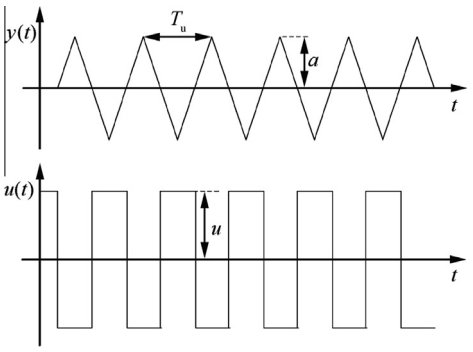

Fig. 4 Oscillation curves of relay output and plant output.

oscillation; ω_u is the frequency of the plant oscillation, defined as ultimate frequency.

In the conventional tuning research, the PI coefficients are then calculated by the Ziegler–Nichols (Z-N) or other improved tuning formulas.[22–24] However, those tuning results cannot always meet the tuning requirements. Research shows that the Z–N tuning formula is inadequate in some case and has to be completely revised[9] because of the limitation of the information recognized from only one critical point.

3.2. Proposed auto-tuning method

The intrinsic idea of the method is to identify the Nyquist point of the plant for the auto-tuning. In Ref. [25], Mattavelli et al. introduced an approach which employs a relay with hysteresis in the closed-loop to identify the Nyquist point. In this paper, the proposed tuning method adds a delay and a filter into the closed-loop so as to indirectly identify the Nyquist point by adding a lag phase to the plant, shown in Fig. 5. The delay time and the filter can be represented as $e^{-\tau s}$ and $1/(T_f s + 1)$,[26] thus the additional part of the transfer function is

$$F(s) = \frac{e^{-\tau s}}{T_f s + 1} \tag{8}$$

where τ is the delay time and T_f is the filter time constant.

The additional part $F(s)$ brings the phase φ_a and the amplitude A_a into the frequency characteristic, which are

$$\varphi_a = -\tau\omega - \arctan(T_f\omega) \tag{9}$$

$$A_a = \frac{1}{\sqrt{1 + (T_f\omega)^2}} \tag{10}$$

It can be derived from Eqs. (9) and (10) that the additional phase is negative, which will cause the phase delay, and the plant amplitude will be reduced.

The first step of the proposed method is to perform the same oscillation experiment as Section 3.1. The ultimate period

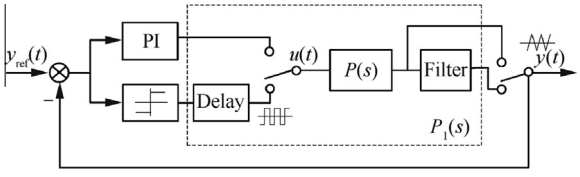

Fig. 5 Block diagram of the proposed tuning method with delay and filter.

T_u and the oscillation amplitude a are measured. The critical point is then derived, which is on the new plant Nyquist curve

$$P_1(s) = F(s)P(s) \tag{11}$$

The critical point contains the information of the plant $P(s)$ and the additional part $F(s)$, and the phase and the amplitude satisfy the equation

$$\begin{cases} \varphi_a + \varphi_\omega = -\pi \\ A_a A_\omega = \left|\frac{1}{N(a)}\right| = \frac{\pi a}{4u} \end{cases} \tag{12}$$

where φ_ω and A_ω are the phase and the margin of the point on plant Nyquist curve.

Considering Eqs. (9), (10) and (12), it is calculated that

$$\begin{cases} \varphi_\omega = -\pi + \tau\omega + \arctan(T_f\omega) \\ A_\omega = \frac{\pi a}{4u}\sqrt{1 + (T_f\omega)^2} \end{cases} \tag{13}$$

Bringing the ultimate frequency ω_u of the oscillation test into the formula, the plant Nyquist point can be derived. ω_u represents the frequency of the Nyquist point.

Consequently, with the plug of the delay time in the relay oscillation, Nyquist point is indirectly located. Likewise, repeating the test with different delay time, more than one critical point can be identified. In this way, the proposed method can get more information of the plant than conventional tuning method.

The second step is to shift the Nyquist point to the position on the unit circle with the specification of the phase margin, through which the PI coefficients are calculated.

The phase and the amplitude of the PI controller are

$$\begin{cases} \varphi_{pi} = -0.5\pi + \arctan(T_i\omega) \\ A_{pi} = \frac{K_p\sqrt{1+(T_i\omega)^2}}{T_i\omega} \end{cases} \tag{14}$$

The final effect of the PI controller is to provide the additional phase and the amplitude in order to shift the proper Nyquist point to the required position. This is mathematically achieved by adding φ_{pi} and multiplying A_{pi} to the Nyquist point, to shift it to the position on the unit circle with a certain phase margin φ_m.

$$\begin{cases} \varphi_\omega + \varphi_{pi} = -\pi + \varphi_m \\ A_{pi}A_\omega = 1 \end{cases} \tag{15}$$

Considering Eqs. ((13)–(15)), the PI coefficients can be derived as

$$T_i = \frac{\tan(0.5\pi + \varphi_m - \tau\omega - \arctan(T_f\omega))}{\omega} \tag{16}$$

$$K_p = \frac{4uT_i\omega}{\pi a\sqrt{\left[1 + (T_f\omega)^2\right]\left[1 + (T_i\omega)^2\right]}} \tag{17}$$

To sum up, the proposed auto-tuning is performed as described in Fig. 6:

(1) Start the tuning and carry out the relay oscillation test with a specific delay time.
(2) Drive the plant to the steady state and obtain a and T_u, locating the critical point A_{crit}.
(3) Calculate the Nyquist point A_{Nyq} from Eq. (13) with the corresponding delay time and the filter time constant. B point shows that the amplitude of A_{Nyq} is changed by the effect of T_f. And the difference of the phase of point B and A_{crit} is φ_a by the effect of τ and T_f.
(4) Shift A_{Nyq} to the tuned point with proper phase margin A_{marg} and calculate the PI coefficients from Eq. (16) with the required phase margin.
(5) Repeat steps (1)–(4) until the required system bandwidth and the damping ratio are obtained.

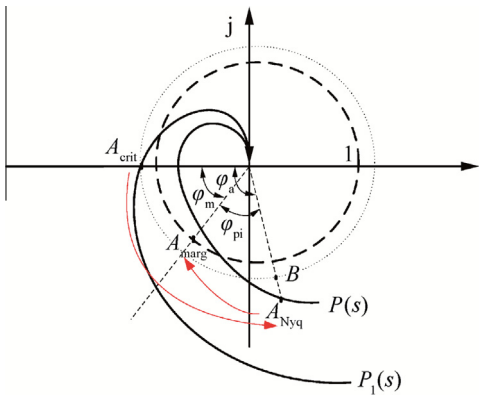

Fig. 6 Sketch of the proposed auto-tuning with delay and filter.

Another discussion is the auto-tuning sequence for the cascade controllers. The PMSM drive system consists of the speed loop and the inner current loop. According to Hang et al.'s research,[27] the current loop performs the relay auto-tuning first and the speed loop is then placed on relay feedback with the current loop closed. Retuning of the current loop is not necessary if the inner loop response is sufficiently faster than the outer loop.

3.3. Definition and setting of the parameters

(1) Filter time constant T_f

The employed first-order low-pass filter is

$$f(s) = \frac{1}{T_f s + 1} \tag{18}$$

The filter is used to eliminate the high-frequency noise in the feedback signal. The bandwidth of the filter must be narrow enough to permit the oscillation recognition, but wide enough to reserve the whole information of the critical point at a frequency higher than the main process dynamics. A good compromise appears to be an automatic determination of T_f so that the corresponding pole in the discrete filter implementation is set to be a chosen real value p_d, that is

$$T_f = -\frac{T_s}{\lg p_d} \tag{19}$$

where the value of p_d adopted is 0.5 and T_s is the sampling time.

In this case, the discrete filter implementation of Eq. (18) employs the same equation in z-domain independent of T_s

$$f(z) = \frac{0.1304(z-1)}{z - 0.7391} \tag{20}$$

(2) Delay time τ

The transfer function of the delay is

$$\tau(s) = e^{-\tau s} \tag{21}$$

The effect of the delay can be explained in both the real-time domain and the s-domain. In the real-time domain, it delays a length of τ and then output the set-point after the moment the feedback signal crosses zero. Obviously the longer the delay, the bigger the oscillation amplitude becomes, and the slower the oscillation frequency goes, which means, a lower frequency Nyquist point is recognized.

In the s-domain, the absolute value of φ_a is proportional to the delay time τ in Eq. (9). The recognized Nyquist point goes counterclockwise on $P(s)$ when φ_a increases, which means a Nyquist point A_{Nyq} of bigger oscillation amplitude and slower frequency is identified. This conclusion accords with the time-domain analysis above.

A further discussion is the relationship between Nyquist point frequency and the system bandwidth ω_n. The bandwidth is the frequency at which the transfer function has -3 dB amplitude. Considering Eqs. (6) and (16), it is derived that

$$\omega_n^2 = \frac{4ku\omega}{\pi a\sqrt{\left[1+(T_f\omega)^2\right]\left[1+(T_b\omega)^2\right]}} \tag{22}$$

where $T_b = K_pT_i$.

This equation shows a connection between ω_n and the Nyquist point frequency. However, the relationship between these frequencies is not immediately evident as it is a transcendental equation. However it can be analyzed geometrically in the s-domain.

Consider $G(s)$ as the open-loop system transfer function which includes the PI controller, the closed-loop system transfer function is

$$\Phi(s) = \frac{G(s)}{1+G(s)} \tag{23}$$

As illustrated in Fig. 7, the amplitude of $\Phi(s)$ is the division of the amplitudes of $|G(s)|$ and $|1 + G(s)|$. $|1 + G(s)|$ can be further expressed as $|G(s) - (-1)|$, which is the length of $\overline{PD}$. $|G(s)|$ equals the length of $\overline{OD}$. Thus the system transfer function is

$$\Phi(s) = \frac{G(s)}{1+G(s)} = \frac{|\overline{OD}|}{|\overline{PD}|}\angle PDO \tag{24}$$

Considering the case where the tuning phase margin is specified as 60°, the length of $|\overline{OD}|$ is equal to $|\overline{PD}|$. Thus at the frequency of the Nyquist point obtained in the oscillation test, the amplitude of $\Phi(s)$ is 1. Also, it is obvious that the higher frequency of the point on Nyquist curve, the smaller the amplitude is, except that there may be a small area on the left side of line l where the $|\overline{OD}|$ is longer than $|\overline{PD}|$ and this is the area containing the resonance frequency. Thus the bandwidth point, whose amplitude is -3 dB, is within the unit circle and has a higher frequency than point D.

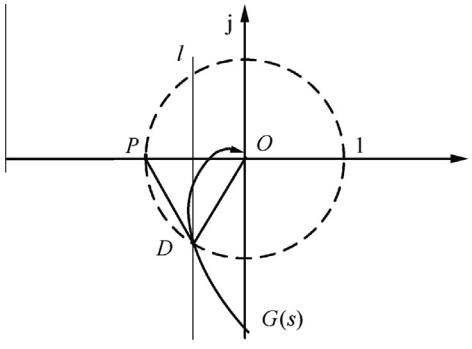

Fig. 7 Illustration of vector on Nyquist curve.

Therefore, the frequency of the recognized point can be considered as a guarantee that the bandwidth is wider than this. The delay time τ can be changed until the frequency of the Nyquist point gets closed to the required system bandwidth.

(3) Phase margin φ_m

The phase margin of the system determines the stability of the dynamic performance. According to the control theory, the bigger the phase margin, the bigger the system damping is, and the smaller overshot the step response is. It can be qualitatively analyzed in Fig. 7 as follows.

The auto-tuning algorithm moves the recognized point to the position on unit circle. $\angle POD$ is the phase margin. Consider the case that $\angle POD$ is 30°, the division of $|\overline{OD}|$ and $|\overline{PD}|$ is bigger than the case when $\angle POD$ is 60°. It is obvious that the amplitude of the area of the natural frequency on the Nyquist curve turns bigger. It will be found in the simulation that the amplitude Bode diagram gets bigger at the frequency area near the natural frequency. Hence the system has a bigger overshoot and a smaller damping ratio in this case. The system response vibrates stronger but rises faster.

The phase margin is mostly set between 30 °and 60°. The bigger the phase margin, the more stable the system becomes but a longer rising time is expected.

4. Simulation and experimental results

4.1. Proposed auto-tuning method simulation results

The auto-tuning method has been studied in Simulink in terms of the transfer function. Two groups of auto-tuning results have been analyzed under the variation of the delay time and the phase margin respectively. Identification of the Nyquist curve verifies the correctness of the auto-tuning theory. The Bode diagram as well as the step response shows the influence on tuning result when the parameters change.

The plant model in the simulation is the first-order model which includes the dead time

$$P(s) = \frac{k}{s+p} \tag{25}$$

where p and k are the parameters of the plant, which are set at 250 and 500, respectively.

First, five oscillation tests are carried out with five different delay time. All the auto-tuning results are calculated when the phase margin is 60°. The data of auto-tuning results with different delay time is shown in Table 1. The frequency of the critical point, the amplitude and the phase of the Nyquist point are listed. The frequency of the critical point is also the frequency of the corresponding Nyquist point. The system bandwidth ω_n is obtained by finding the -3 dB point in Bode diagram. The damping ratio is calculated from Eq. (10). It can be seen that with the increase of the delay time, the frequency of the Nyquist point identified gets smaller. The bandwidth

Table 1 Tuning results with different delay time ($\varphi_m = 60°$).

τ (μs)	ω (Hz)	A_ω	φ_ω (rad)	ω_n (Hz)	ς	K_i	K_p
80	781.25	0.1307	−1.8293	886.9	2.416	1331	7.383
240	520.83	0.2052	−1.6377	598.7	1.360	1606	4.373
400	390.63	0.2757	−1.5794	436.3	1.098	1388	3.157
560	312.50	0.3491	−1.5588	342.3	0.971	1164	2.463
720	271.74	0.4048	−1.4842	300.9	0.817	1193	2.024

and the damping ratio also change monotonically. The tuning performance is related to the setting of the delay time.

The corresponding frequency and the real-time response of the tuning result with different delay time in Table 1, are shown in Fig. 8 which is the Bode diagram and Fig. 9, which is assumed of I tuning for current loop. The -3 dB frequency point is moving towards the low frequency side, when the delay time increases, which means that the bandwidth is getting smaller.

An estimated value of the rising time and the settling time is

$$\begin{cases} t_r = \dfrac{3\varsigma}{\omega_n} \\ t_s = \dfrac{4}{\varsigma\omega_n} \end{cases} \tag{26}$$

Accordingly, in the step response the settling time gets longer when both ς and ω_n become smaller. The overshoot is getting bigger due to the reduction of ς. The long delay time results in the slow system step response. Therefore, it is concluded that the longer the delay time, the smaller the bandwidth becomes.

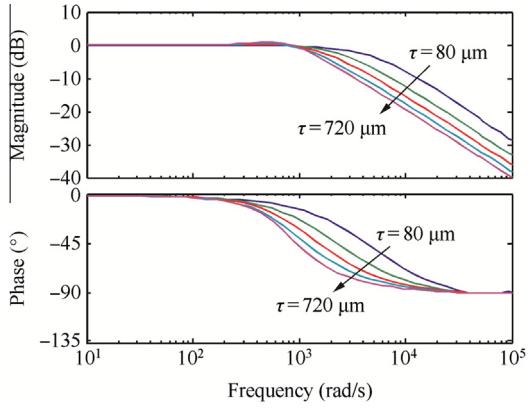

Fig. 8 Bode diagram of tuning results with different delay time.

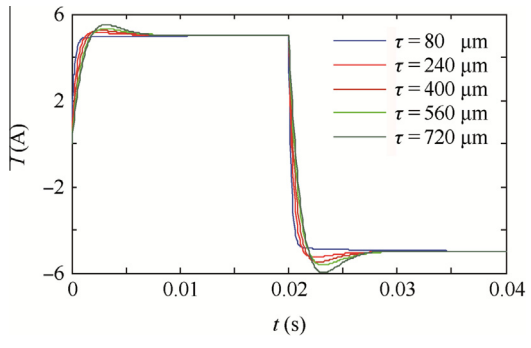

Fig. 9 Step response of tuning results with different delay time.

In order to prove the validity of the auto-tuning method, those five identified Nyquist points are illustrated in contrast with the actual Nyquist curve of the plant. The position of the Nyquist points (the red stars) are illustrated in Fig. 10 with the amplitude and the phase in Table 1, while the blue curve is the actual plant Nyquist curve from Eq. (25). It can be found that the identified Nyquist points go counterclockwise almost along the Nyquist curve. Fig. 10 shows a good accordance of the tuning method. It shows that by injecting some certain delay time, a Nyqusit point is selected and indirectly identified by identifying the relay oscillation point.

Secondly, the auto-tuning results with different phase margins for one critical point are shown in Table 2. The critical point is the oscillation result when the time delay is 400 μs, and the amplitude and the phase can be found in Table 1. The bandwidth slowly increases and the damping ratio falls significantly, when the phase margin reduces from 60° to 30°.

The corresponding frequency and the real-time response, with different phase margins, are shown in Fig. 11 which is the Bode diagram and Fig. 12. It can be seen in Table 2 that the damping ratio falls from 1.097 to 0.406. The highest amplitude in Bode diagram in Fig. 11 increases to almost 4 dB at the phase margin of 30°. However, the frequency of -3 dB point does not change significantly, which indicates that the phase margin is more related to the system damping ratio.

In Fig. 12, the step response is shown. The rising time slightly reduces but the settle time is getting longer due to the reduction of ς in Eq. (26). The vibration is also getting larger. Hence, it shows that the tuning phase margin determines the damping ratio of the system.

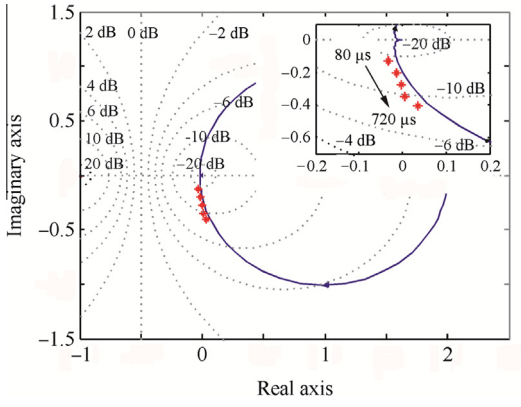

Fig. 10 Contrast of the identified Nyquist points and actual Nyquist curve.

Table 2 Auto-tuning results with different phase margins for one critical point.

φ_m (°)	ω_n (Hz)	ς	K_i	K_p
60.0	437.4	1.097	1388	3.157
52.5	470.1	0.884	1848	2.897
45.0	489.2	0.703	2409	2.588
37.5	513.9	0.546	3138	2.234
30.0	546.5	0.406	4161	1.842

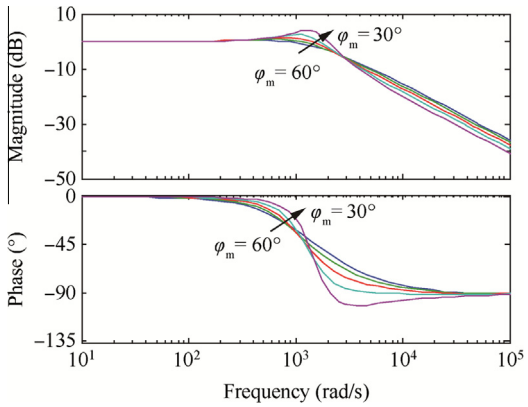

Fig. 11 Bode diagram of tuning results with different phase margins.

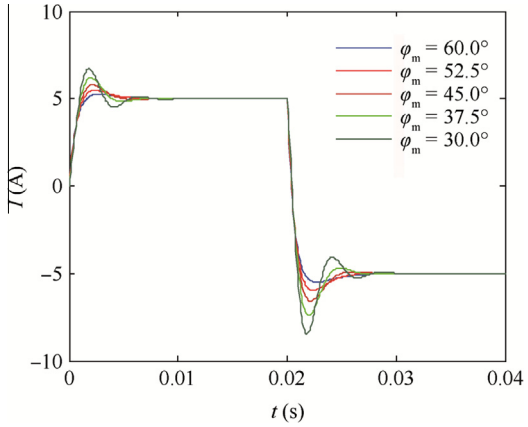

Fig. 12 Step response of tuning results with different phase margins.

4.2. Experimental setup and results

The proposed relay auto-tuning method has been validated with an experimental setup consisting of an indirect matrix converter[28,29] PMSM drive. The PI controller scheme with output saturation and anti-windup features is the same as the one when knowing the parameters of the plant. Only the K_p and K_i need to be tuned for the PI controller.

Two different machines were considered for the experimental validation, a 10-pole pair PMSM and a 7-pole pair PMFSM[30] (controlled as a PMSM). Each of the two motors was designed and manufactured by the Power Electronics, Machines and Control Group, University of Nottingham. It has been demonstrated that field-oriented control can be employed on a PMFSM[31,32] and therefore be seen from the controller side, the PMFSM is controlled in the same way as the PMSM. The parameters (inductance, resistance, inertia and friction) of the two motors are unknown.

The core controller is based on a Texas Instruments TMS320C6713 plus Actel A3P400 FPGA. The auto-tuning method is implemented in the digital signal process (DSP) and Matlab on a PC. The communication between DSP and PC uses a USB data connection. The experimental setup, including PMFSM and DC load motor and the indirect matrix converter, are shown in Fig. 13.

Since the Bode diagram cannot be illustrated without the parameters of the plant, the step response of the tuning results is provided to show the validity of the tuning method. The sampling time of the current loop and the speed loop is 80 μs and 4 ms, respectively.

The PI controller of both the current loop (*d*-axis) and the speed loop can be tuned with the auto-tuning technique. Since the bandwidth of the current loop is around several hundred Hertz whereas the speed loop is several Hertz or tens Hertz, the current loop response can be considered to be much faster and it can therefore be ignored during the speed loop tuning. The outputs of the tuning relay are ±5 A and ±100 r/min, respectively.

The PMSM is tuned first. Fig. 14(a) shows the step response of the current loop for *I* at 60° phase margin with different delay time. As the delay time is increased from 240 μs to 720 μs, the overshoot of the step response gets larger and the steady state settling time is increased. The increasing overshoot is caused by a reduction in the damping ratio and the longer settle time is the result of a smaller bandwidth; these results are the same as those found in the simulation.

Compared to the simulation results, the trend of the increasing delay time seems different in the experiment, which can be explained as follows. Both ς and ω_n reduce as the delay time gets longer. According to Eq. (26), the rising time will increase if ς reduces much slowly than ω_n as shown in the simulation results, whereas it will decrease if ς reduces faster than ω_n as shown in the experiment results.

Fig. 14(b) shows the step response of the current loop at different phase margins. With a decrease in the phase margin

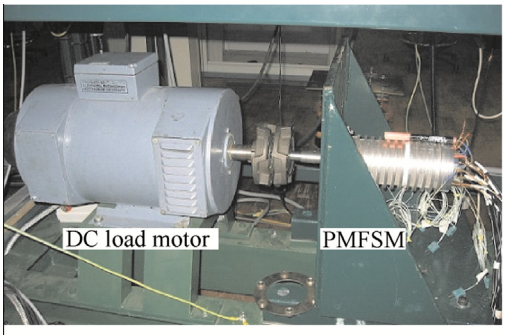

(a) PMFSM and DC load motor

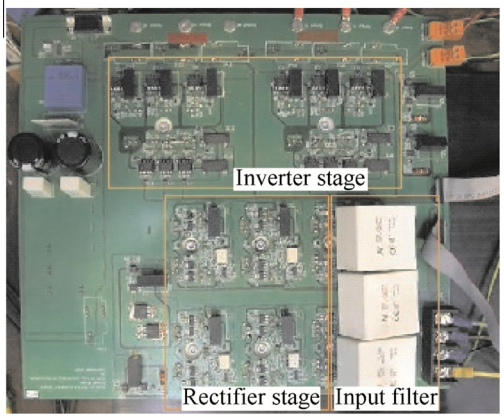

(b) Indirect matrix converter

Fig. 13 Experimental setup.

from 60° to 30°, the damping ratio becomes smaller. It is also clear that the vibration around the set-value becomes larger, the same conclusion as shown in the simulation result.

The speed loop for n is tuned after the faster, inner current loop is tuned. The tuning result of the speed loop is similar to the result of the current loop. In Fig. 15(a), with an increase of the delay time, the step response oscillation is larger and the settling time becomes longer, implying a decrease of the system bandwidth and the damping ratio. In Fig. 15(b), the decrease of the phase margin results in a smaller damping ratio, which results in larger oscillation around the set point value and faster rising time. Another caveat is that the noise of the speed curve is due to the limited resolution of the resolver.

The tuning algorithm was then run on the PMFSM. Fig. 16 shows the auto-tuning results of the current loop with different delay time. Since the current loop is much faster than the speed loop, the stability is considered to be more important than the rising time. The overshoot should be controlled to a reasonable level. Therefore the tuning phase margin is set to 60°. The response of the tuning result under 80 μs is over-damped whereas the oscillation is too large for a delay under 240 μs. Consequently, the tuning result for 160 μs is employed as the PI coefficients.

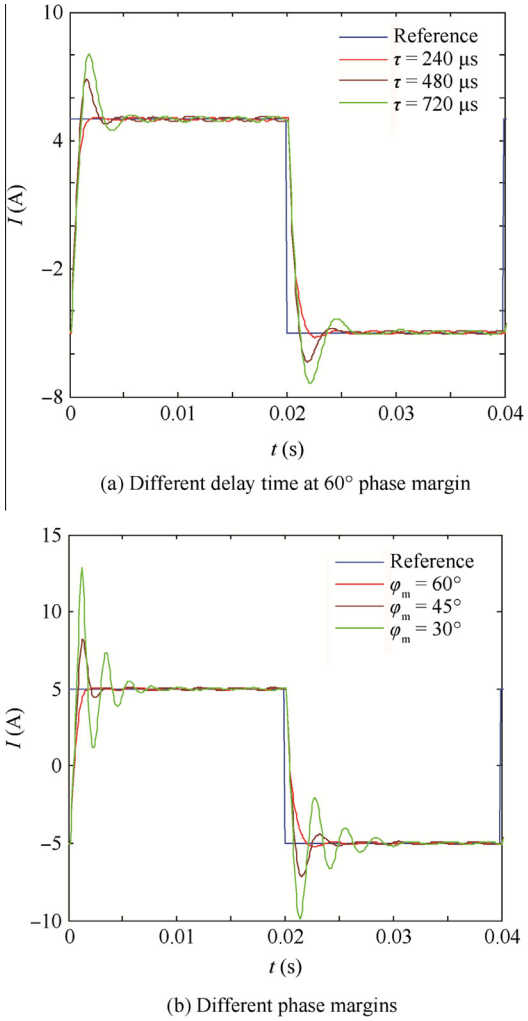

Fig. 14 Step response of current loop auto-tuning experiment on PMSM.

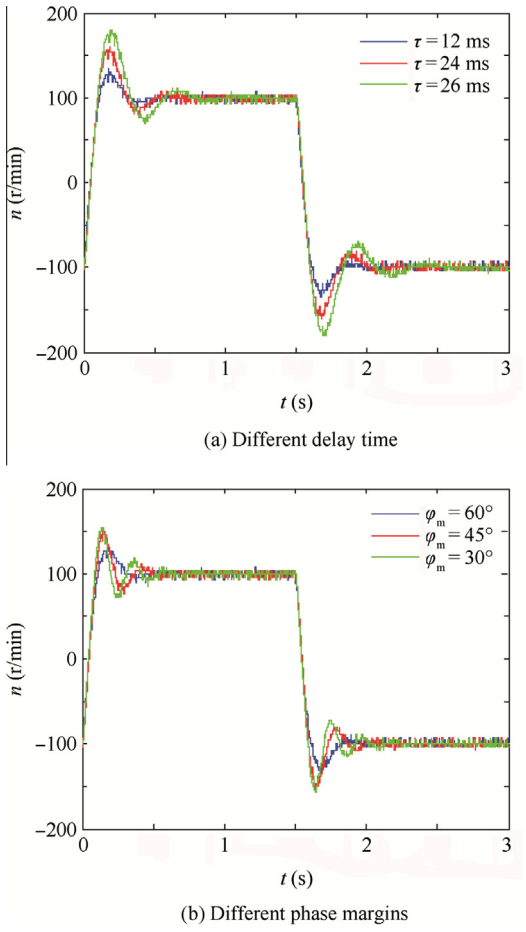

Fig. 15 Step response of speed loop auto-tuning experiment on PMSM.

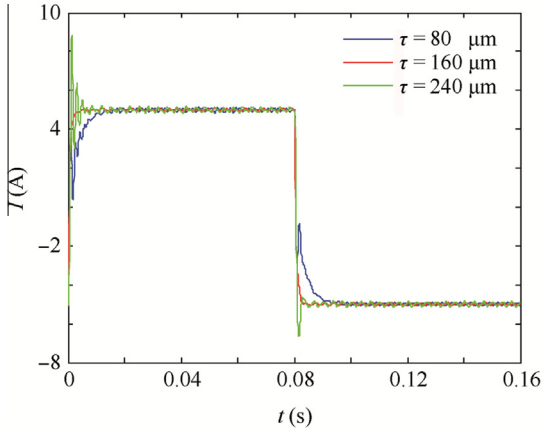

Fig. 16 Auto-tuning results of the current loop with different delay time.

The changing of the system inertia is the main reason for implementing PI auto-tuning. In order to show the validity of the tuning method, the speed loop is tuned with different system inertias by connecting or disconnecting the plant motor to the load DC motor. The DC motor works in the generating mode with its armature connected to a load resistance. The DC

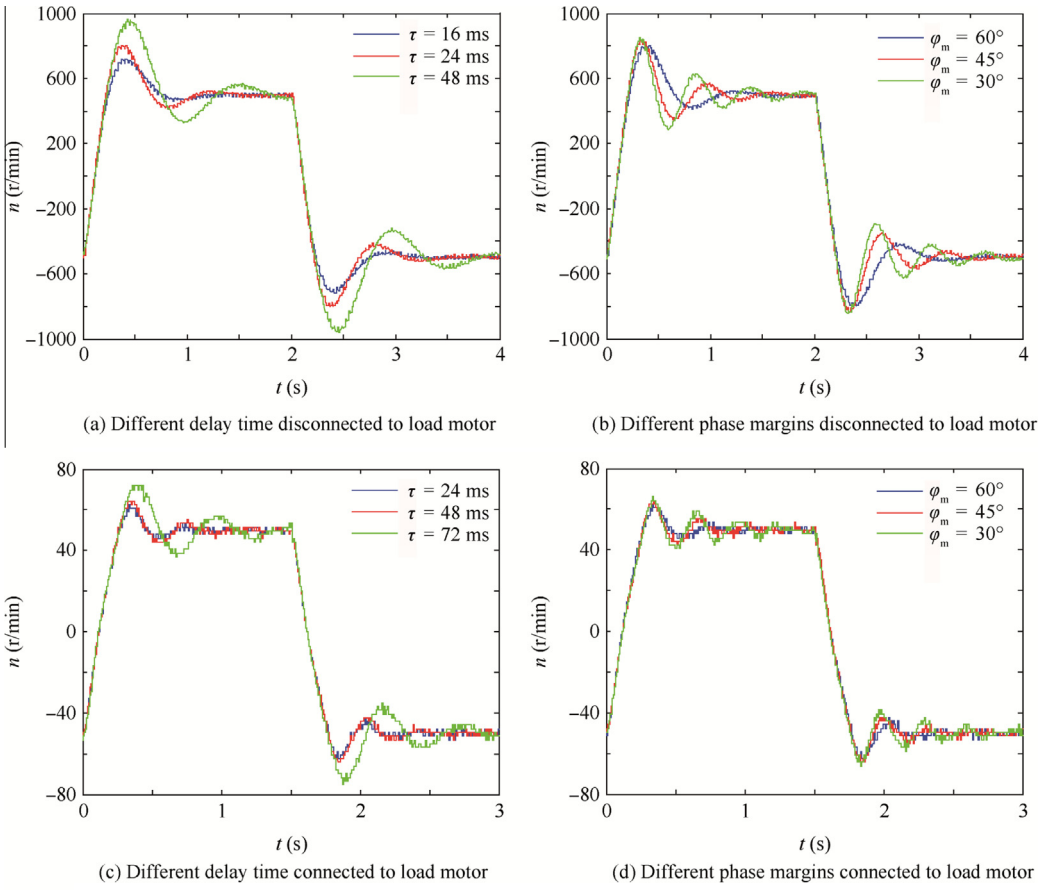

Fig. 17 Step response of speed loop auto-tuning experiment on PMFSM.

motor is a high-inertia and low-speed motor. The limitation of the speed is 500 r/min.

Figs. 17(a) and (b) show the step response of the auto-tuning results when the PMFSM is not connected to the DC motor. The speed reference is set to 500 r/min. The oscillations are greater and settling time longer when the delay time increases, and it oscillates larger and rises faster as the phase margin reduces, the same conclusion as in PMSM tuning in Fig. 14. The rising time is around 0.25 s when the speed reaches 500 r/min and is around 0.10 s when the speed reaches 50 r/min.

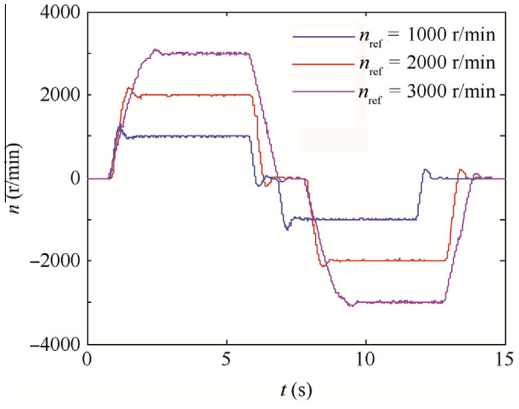

Fig. 18 Response of speed loop auto-tuning with different speeds.

Figs. 17(c) and (d) show the tuning results when the PMFSM is connected to the DC motor. The speed reference is set to 50 r/min, because of the limitation of the DC motor. The rising time is up to 0.25 s when the speed reaches 50 r/min, longer than rising time of 0.10 s when the DC motor is not connected. It is because the highest torque of the PMFSM is constant due to the current limitation of the IGBT and the armature, but the inertia increases when the DC motor is connected. The changing of rising time and vibration is similar to the trend in Fig. 17(a) and (b) for different delay time and different phase margins. The auto-tuning method successfully tuned the PI controller with DC motor connected or disconnected to the PMFSM.

Fig. 18 shows the speed response of 1000 r/min, 2000 r/min and 3000 r/min, at the same PI auto-tuning parameters. The slope of the rising speed is concerned with the saturation of the current limit. This figure verifies the auto-tuning results for a wide speed range.

The above discussion leads to the conclusion that the experimental results agree with the simulation analysis. The proposed auto-tuning method finds valid PI coefficients and provides different results for ς and ω_n with the specification of τ and φ_m. The most satisfactory tuning result can be chosen from the result presented in Fig. 17.

5. Conclusions

(1) This paper presents a PI auto-tuning algorithm based on the relay oscillation test, providing different system performances which depend on the setting of the delay time and the phase margin.
(2) The ultimate goal of this research is to allow non-experts to utilize the existing knowledge in the area of the PI controller and to provide intelligent and fast tuning procedures for the current loop and the speed loop.
(3) The theory of the proposed auto-tuning method is studied and verified in the simulation. The method has been tested on two PMSMs.
(4) The experimental results show the validity of the method and the tuning method provides different tuning results for the system bandwidth and the damping ratio.

Acknowledgements

The authors would like to acknowledge part funding for this work from the Clean Sky JTI – Systems for Green Operations ITD. This work was supported by the National Natural Science Foundation of China (No. 50807002), the Aeronautical Science Foundation of China (No. 2008ZC51045) and the Beijing Nova Program (No. 2008B13).

References

1. Levi E, Jones M, Vukosavic SN. A series-connected two-motor six phase drive with induction and permanent magnet machines. *IEEE Trans Energy Convers* 2006;**21**(1):121–9.
2. Guo H, Xing W. Development of electromechanical actuators. *Acta Aeronaut Astronaut Sin* 2007;**28**(3):620–7 [Chinese].
3. Mohamed YAI. Adaptive self-tuning speed control for permanent-magnet synchronous motor drive with dead Time. *IEEE Trans Energy Convers* 2006;**21**(4):855–62.
4. O'Mahony T. PID tuning software: a practical review. *Proceedings of IET Irish signals and systems conference*; 2006 Jun 28–30; Dublin, Ireland; 2006. p. 409–14.
5. Panda RC, Yu CC, Huang HP. PID tuning rules for SOPDT systems: review and some new results. *ISA Trans* 2004;**43**(2):283–95.
6. Ziegler JG, Nichols NB, Rochester NY. Optimum settings for automatic controllers. *Trans Am Soc Mech Eng* 1942;**64**:759–68.
7. Cohen GH, Coon GA. Theoretical considerations of retarded control. *Trans Am Soc Mech Eng* 1953;**75**:827–34.
8. Åström KJ, Hägglund T. Automatic tuning of simple controllers with specification on phase and amplitude margins. *Automatica* 1984;**20**(5):645–51.
9. Hang CC, Astrom KJ, Ho WK. Refinements of the Ziegler–Nichols tuning formula. *IEE Proc D Control Theory Appl* 1991;**138**(2):111–8.
10. Chen YQ, Moore KL. Relay feedback tuning of robust PID controllers with iso-damping property. *IEEE Trans Syst Man Cybernet – Part B: Cybernetics* 2005;**35**(1):23–31.
11. Chen D, Segorg DE. PI/PID controller design based on direct synthesis and disturbance rejection. *Industr Eng Chem Res* 2002;**41**(19):4807–22.
12. Silva GJ, Datta A, Bhattacharrya SP. New results on the synthesis of PID controllers. *IEEE Trans Autom Control* 2001;**47**(2):241–52.
13. Kshirsagar P, Burgos RP, Lidozzit A, Jang J, Wang F, Boroyevich D, et al. Implementation and sensorless vector-control design and tuning strategy for SMPM machines in fan-type applications. *Proceedings of 2006 IEEE industry applications conference*; 2006 Oct 8–12;Tampa, FL. Piscataway, NJ:IEEE; 2006. p. 2062–9.
14. Hang CC, Astrom KJ, Wang QG. Relay feedback auto-tuning of process controllers-tutorial review. *J Process Control* 2002;**12**(1):143–62.
15. Wang QG, Hang CC, Zou B. A frequency response approach to auto-tuning of multivariable controllers. *Chem Eng Res Des* 1997;**75**(8):797–806.
16. Hang CC, Wang QG, Cao LS. Self-tuning Smith predictors for processes with long dead time. *Int J Adapt Control Signal Process* 1995;**9**(3):255–70.
17. Park JH, Sung SW, Lee IB. Improved relay auto-tuning with static load disturbance. *Automatica* 1997;**33**(4):711–5.
18. Wang QG, Lee TH, Zhang Y. Multi-loop version of the modified Ziegler–Nichols method for TITO processes. *Ind Eng Chem Res* 1998;**37**(12):4725–33.
19. Shen ZQ, Wang LN, Xiao K. Relay auto-tuning of two-stage matrix converter based PMSM drives. *Proceedings of 2011 international conference on electrical machines and systems*; 2001 Aug 20–23; Beijing. Piscataway, NJ: IEEE; 2001. p. 1–4.
20. Hägglund T, Åström KJ. Industrial adaptive controllers based on frequency response techniques. *Automatica* 1991;**27**(4):599–609.
21. Åström KJ, Hägglund T. *PID controllers: theory, design, and tuning*. 2nd ed. Research Triangle Park, NC: Instrument Society of America; 1995.
22. Schei TS. A method for closed loop automatic tuning of PID controllers. *Automatica* 1992;**28**(3):587–91.
23. Wang QG, Hang CC, Bi Q. Process frequency response estimation from relay feedback. *Control Eng Practice* 1997;**5**(9):1293–302.
24. Sung SW, Lee IB, Lee J. New process identification method for automatic design of PID controllers. *Automatica* 1998;**34**(4):513–20.
25. Mattavelli P, Tubiana L, Zigliotto M. Simple control autotuning for PMSM drives based on feedback relay. *European conference on power electronics and applications*; 2005; Dresden, Germany: 2005. p. 1–10.
26. Leva A. PID autotuning algorithm based on relay feedback. *IEE Proc D Control Theory Appl* 1993;**140**(5):328–38.
27. Hang CC, Loh AP, Vasnani VU. Relay feedback auto-tuning of cascade controllers. *IEEE Trans Control Syst Technol* 1994;**2**(1):42–5.
28. Kumar D, Wheeler P, Clare J. Experimental evolution of the multi-drive system based on two-stage direct power converter topology. *Proceedings of 2010 14th international power electronics and motion control conference*; 2010; Ohrid, Macedonia: 2010. p. T5-207–12.
29. Kolar JW, Friedli T, Rodriguez J, Wheeler PW. Review of three-phase PWM AC-AC Converter Topologies. *IEEE Trans Industr Electron* 2011;**58**(11):4988–5006.
30. Raminosoa T, Gerada C, Galea M. Design considerations for a fault-tolerant flux-switching permanent-magnet machine. *IEEE Trans Industr Electron* 2011;**58**(7):2818–25.
31. Hua W, Cheng M, Lu W, Jia HY. A new stator-flux orientation strategy for flux-switching permanent magnet motor based on current-hysteresis control. *J Appl Phys* 2009;**105**(7):1–3, 07F112–07F112-3.
32. Cai YH, Qi RY, Cai J, Deng ZQ. Online modeling for switched reluctance motor using radial basis function neural network and its experimental validation. *Acta Aeronaut Astronaut Sin* 2012;**33**(4):705–14 [Chinese].

Wang Lina is an associate professor and master supervisor at school of automation science and electrical engineering, Beihang University. Her current research interests are power electronics and motor control.

Xiao Kun received his Ph.D. degree in electrical engineering from Beihang University in 2012, and then works in State Grid DC Project

Construction Company Limited. His main research interests are high-voltage direct current (HVDC) and power electronics.

Liliana de Lillo is a senior research fellow in faculty of engineering, University of Nottingham. Her area of research includes matrix converters, power electronics and power device.

Lee Empringham is a senior research fellow in faculty of engineering, University of Nottingham. His research area includes power electronics and power device.

Pat Wheeler received his Ph.D. degree in electrical engineering for his work on Matrix Converters at the University of Bristol, England in 1993. In 1993, he moved to the University of Nottingham and worked as a research assistant in the School of Electrical and Electronic Engineering. In 1996, he became a lecturer in power electronic systems with the Power Electronics, Machines and Control Group at the University of Nottingham, UK, became a senior lecturer in 2003, and a professor in January 2008. He now works as the director of the institute for aerospace technology and professor of power electronic systems, faculty of engineering, University of Nottingham.